

Short communication

Synthesis and characterization of $\text{Li}_2\text{MnSiO}_4/\text{C}$ nanocomposite cathode material for lithium ion batteries

Yi-Xiao Li, Zheng-Liang Gong, Yong Yang*

State Key Lab for Physical Chemistry of Solid Surfaces and Department of Chemistry, Xiamen University, Xiamen 361005, China

Available online 27 June 2007

Abstract

A high capacity $\text{Li}_2\text{MnSiO}_4/\text{C}$ nanocomposite cathode material with good rate performance for lithium ion batteries through a solution route has been successfully prepared. The material is able to deliver a reversible capacity of 209 mAh g^{-1} in the first cycle, i.e. more than one electron exchange can be reversible cycled in the materials. The highly dispersion of nanocrystalline $\text{Li}_2\text{MnSiO}_4$ which was surrounded by a thin film of carbon was attributed to the cause of excellent performance of the materials. Ex situ XRD and IR results show that poor cycling behavior of $\text{Li}_2\text{MnSiO}_4$ might be due to an amorphization process of the materials.

© 2007 Published by Elsevier B.V.

Keywords: Cathode materials; Dilithium manganese silicates; Lithium ion battery; Nanocomposites; Synthesis

1. Introduction

Lithium ion batteries are key components for providing electricity in portable entertainments, telecommunications and computing devices in the 21st century [1]. Although the lithium battery industry has already become one of the largest segments of the portable battery industry and has dominated the laptop computer, cell phone, and camera power source industry, its further exploitation has been limited by the choice of suitable cathode materials. For the most widely used active cathode material today, e.g. LiCoO_2 , a growing concern is on its environmental and toxic hazards associated with cobalt. And the scarcity of cobalt makes it too expensive to be used in large batteries for transportation applications. Safety is another critical issue remained partly unsolved, as this lithiated metal oxide material may act as a strong oxidizer at highly charged state while contacting with an organic electrolyte [2]. The discovery of lithium iron phosphate (LiFePO_4) [3] has changed the Li ion battery landscape in this context. This is the first cathode material with potentially low cost, high thermal stability and also environmentally benign. On the other hand, this cathode suffers from the high rate capability due to its diffusion-controlled kinetics of the elec-

trochemical process duly limited by intrinsic poor electronic conductivity.

Silicon is an element with natural abundance and non-toxic characteristics. And orthosilicate is one class of the attractive polyanions with intrinsic thermal stability. Recently some reports [4–9] have indicated that silicates might be developed as a new class of cathode materials; nevertheless, they were found to suffer from the same drawback of poor electronic conductivity and poor rate performance as LiFePO_4 . It should be emphasized, however, that one of the outstanding properties of orthosilicates such as Li_2MSiO_4 is that exchange of two electrons per transition metal atom (M) is possible. Hence the theoretical capacity of Li_2MSiO_4 can reach as high as 330 mAh g^{-1} (e.g. 333 for $\text{M} = \text{Mn}$; 325 for $\text{M} = \text{Co}$; and 325.5 mAh g^{-1} for $\text{M} = \text{Ni}$). This is significantly superior to the corresponding LiMPO_4 where usually only one electron exchange is available with the theoretical capacity of only 170 mAh g^{-1} ; and is also much higher than that of the commercialized LiCoO_2 of 274 mAh g^{-1} . Unfortunately, normally only about 0.7 electron exchange could be practically realized, demanding for new technology to improve the performance of these silicate materials.

Herein we report a novel approach for the synthesis of a $\text{Li}_2\text{MnSiO}_4/\text{C}$ nanocomposite material based on a solution route. The as-prepared material shows a reversible discharge capacity as high as 209 mAh g^{-1} with an excellent rate performance as contrasted to that reported for the silicate materials [4–7]. This is the first time that more than one electron exchange is actually

* Corresponding author.

E-mail address: yyang@xmu.edu.cn (Y. Yang).

cycled reversibly in the silicate cathode materials. In addition, a possible fading mechanism of the $\text{Li}_2\text{MnSiO}_4$ material during charge and discharge cycles is provided in this work.

2. Experimental

The $\text{Li}_2\text{MnSiO}_4/\text{C}$ composite was prepared by mixing $\text{LiAc}\cdot 2\text{H}_2\text{O}$, $\text{Mn}(\text{Ac})_2\cdot 2\text{H}_2\text{O}$ and $\text{Si}(\text{OC}_2\text{H}_5)_4$ in a water–ethanol system. The mixture was stirred at 80°C for 24 h in a reflux system and then dried at 120°C . After cooling to room temperature, the mixture was milled with sucrose in acetone (for preparation of pure $\text{Li}_2\text{MnSiO}_4$, this process is omitted). After evaporating of acetone, the mixture was pressed into pellets and heated to 600°C for 10 h in a flow of N_2 . Lithium and manganese were determined by ICP-AES (IRIS Intrepid II XSP, Thermo Electron, USA), and silicon by chemical analysis. Element analysis showed the molar ratio of Li:Mn:Si was approximately 1.95:1.00:1.02, which is consistent with the chemical formula of $\text{Li}_2\text{MnSiO}_4$. The carbon content in the composites was determined to be 9.1 wt% (EA1110 ThermQuest Italia S.P.A., Italy). The XPS spectra were measured on a Quantum 2000 spectrometer (Physical Electronics, USA). The morphology of the sample was characterized by HRTEM technique on Tecnai F30 (Philips-FEI, Netherlands). The XRD patterns were measured using $\text{Cu K}\alpha$ radiation on a Panalytical X'Pert (Philip, Netherlands) instrument. The IR spectra were measured on a Nicolet Avatar 360 FTIR instrument with an infrared microscope and ATR accessory (Thermo-electro., USA). Cathodes were fabricated by mixing the materials with 10% acetylene black and 10% polyvinylidene fluoride (PVDF) binder, and pasted on aluminum current collector. Electrochemical performance of the cathode was evaluated at room temperature by coin-type cells using a non-aqueous electrolyte (1 M $\text{LiPF}_6/\text{EC-DMC}$ 1:1 wt%) with Li foils as the anodes. All of the data of specific capacity were calculated with mass of $\text{Li}_2\text{MnSiO}_4$, not including carbon content. Other details of electrochemical measurements and treatment of electrodes

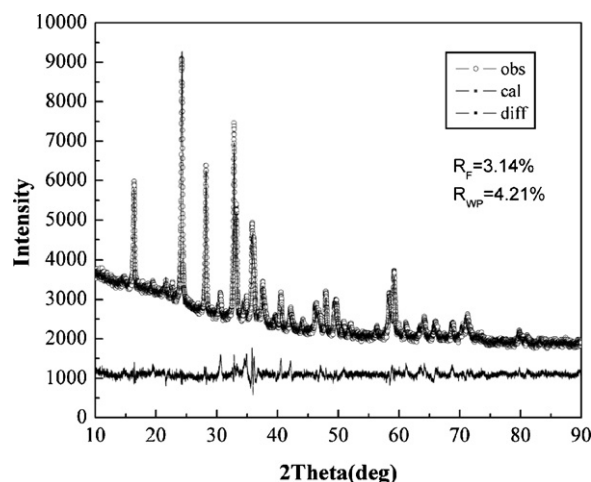


Fig. 1. XRD pattern and Rietveld plot of $\text{Li}_2\text{MnSiO}_4$. Cycles are experimentally measured XRD patterns, upper line is the calculated pattern and lower line is the difference curves between experimental and calculated pattern. The residual factors R_F and R_{WP} are also shown in the figure.

for ex situ experiments can be found in our previous work [10].

3. Results and discussion

Fig. 1 shows that XRD pattern, Rietveld plot of $\text{Li}_2\text{MnSiO}_4$ and the calculated atomic parameters are shown in Table 1. The crystal system is shown to be orthorhombic and the space group is $Pmn2_1$. Cell parameters refined by the Rietveld method using GSAS software are $a = 6.308(3) \text{ \AA}$, $b = 5.377(7) \text{ \AA}$, and $c = 4.988(9) \text{ \AA}$. The X-ray diffraction (XRD) pattern suggests that $\text{Li}_2\text{MnSiO}_4$ be isostructural with $\text{Li}_2\text{FeSiO}_4$ [4,6,7]. This is consistent with the crystal structure of $\text{Li}_2\text{MnSiO}_4$ firstly reported by Setoguchi [11].

In order to confirm that pure $\text{Li}_2\text{MnSiO}_4$ has been synthesized, several spectroscopic techniques have been used for the characterization of the samples. Fig. 2 shows the X-ray photo-

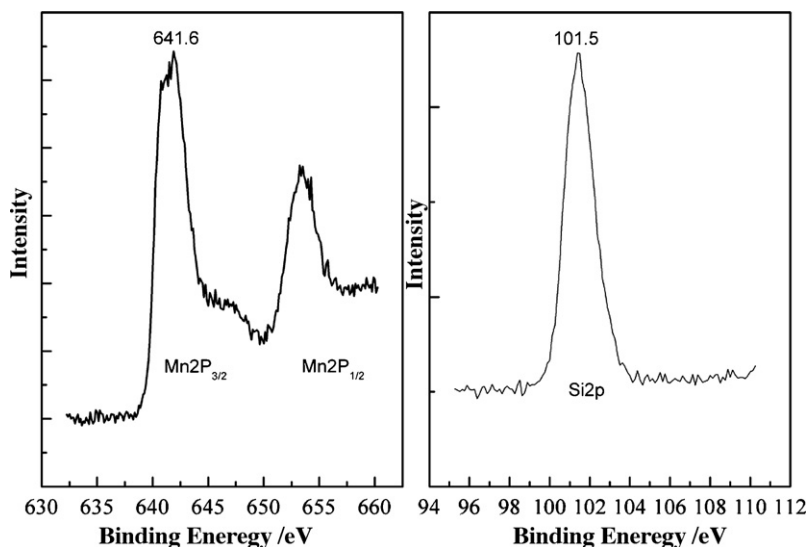


Fig. 2. Mn 2p and Si 2p XPS spectra of $\text{Li}_2\text{MnSiO}_4$ material.

Table 1

Atomic parameters of $\text{Li}_2\text{MnSiO}_4$ calculated from experimental XRD and Rietveld refinement software

Label	<i>x</i>	<i>y</i>	<i>z</i>
Li	0.2031	0.2998	0.8834
Mn	0.5	0.8237	0.9764
Si	0	0.8336	0
O1	0.2212	0.6571	0.8925
O2	0	0.1111	0.9509
O3	0.5	0.2125	0.8562

electron spectroscopy (XPS) of the material. The binding energy of Mn 2p_{3/2} (641.6 eV) is consistent with that of Mn²⁺ of MnO [12], showing that the oxidation state of manganese in our samples is Mn²⁺. The binding energy of Si 2p (101.5 eV) is in line with that of Si⁴⁺ in Ca₂SiO₄ [13], indicating the formation of the orthosilicate structure [SiO₄].

Fig. 3 shows a typical HRTEM image of the $\text{Li}_2\text{MnSiO}_4/\text{C}$ nanocomposite material. It is shown that the crystalline $\text{Li}_2\text{MnSiO}_4$ particles are surrounded by a very thin film of amorphous carbon. The particle size is only tens of nanometers, which means a short diffusion path of lithium ions and good electronic conductivity of the composite materials could be achieved. Thus the transportation of both electron and lithium ion should be easy in the composite material and good rate performances of the composite materials could be expected.

Fig. 4 shows the electrochemical performances of the material. When cycled at room temperature between 1.5 and 4.8 V at a current density of 5 mA g⁻¹, the material gave an initial charge capacity of 310 mAh g⁻¹ (ignoring the side-reaction, about 93% of the theoretical capacity of the material). The first discharge capacity was 209 mAh g⁻¹ (about 63% of the theoretical capacity of the material, 1.25 electrons per unit formula were exchanged). These results clearly demonstrated that more than one electron exchange occurred in the as-prepared material, leading to an enhanced capacity of the $\text{Li}_2\text{MnSiO}_4$ cathode. In addition, when charged/discharged at different current densities (discharge curves are shown in Fig. 4C), the first discharge capacity of the material changed from 209 mAh g⁻¹ at 5 mA g⁻¹ to 135 mAh g⁻¹ at 150 mA g⁻¹. Thus an increase in the charge/discharge current density did not lead to a large decrease in capacity. This is quite different from a very recent report for $\text{Li}_2\text{VOSiO}_4$ [5], where an increase in the discharge rate led to a dramatic decrease in capacity. We also found that $\text{Li}_2\text{MnSiO}_4$ without carbon only delivered a very low discharge capacity (about 10 mAh g⁻¹, not shown here), indicating that the electronic conductivity of the as-made composite material has been greatly improved by the addition of carbon with our method.

Fig. 4A shows that the first charge curve of the material is quite different from the ones followed. The cycling performance shown in Fig. 4B reveals that the discharge capacity decreased sharply from 209 mAh g⁻¹ (1.25 electron) on the first cycle down to 140 mAh g⁻¹ (0.84 electron) on the 10th cycle. In order to understand the fading mechanism of the $\text{Li}_2\text{MnSiO}_4$ material, ex situ XRD and IR were carried out on the first cycle, with

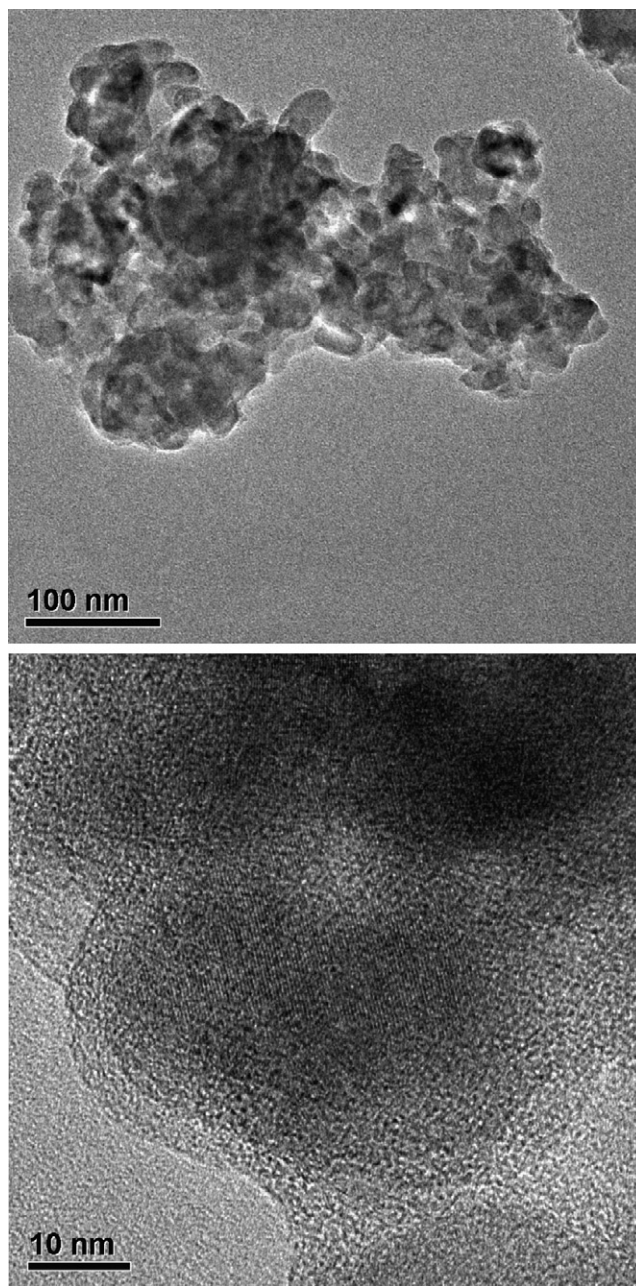


Fig. 3. HRTEM images of $\text{Li}_2\text{MnSiO}_4/\text{C}$ nanocomposite material with different magnifications.

the electrodes charged or discharged to different potentials at a current density of 30 mA g⁻¹.

Fig. 5A shows that how the XRD patterns of the electrodes changed after being charged or discharged to different voltages on the first cycle in a coin cell. From Fig. 5A, it is clear that when the cell was charged to 4.2 V, the typical diffraction peaks associated with the crystal $\text{Li}_2\text{MnSiO}_4$ were much weaker than those of the uncharged one. And when charged to 4.5 and 4.8 V, the peaks can barely be observed. Further more, no strong peaks associated with the crystal $\text{Li}_2\text{MnSiO}_4$ can be observed when the electrodes are discharged to 3.2, 2.8 or 1.5 V. Here we should point out that the peak around 38° (2θ) is attributed to the aluminum current collector for the electrodes. Fig. 5B

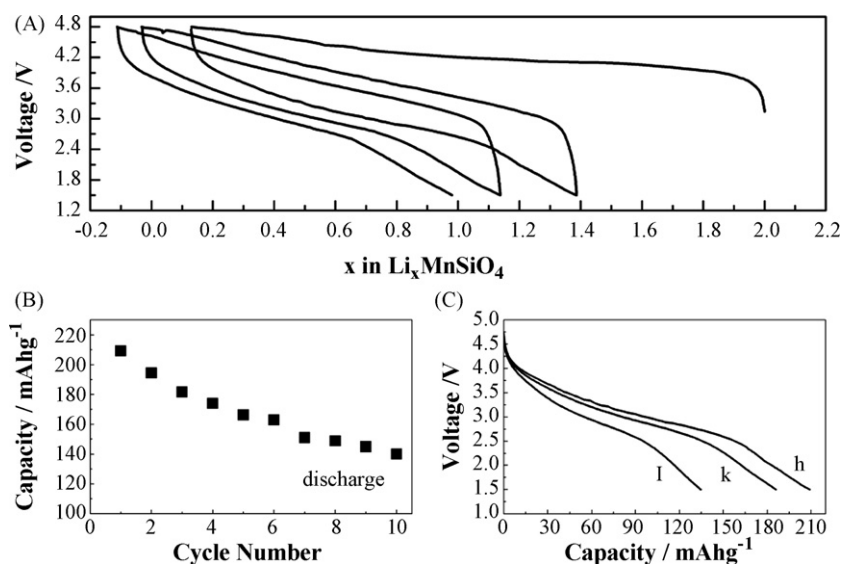


Fig. 4. Electrochemical performances of the material: (A) voltage vs. composition curves at 5 mA g^{-1} ; (B) cycling performance between 1.5 and 4.8 V at 5 mA g^{-1} ; (C) first discharge curves at different current densities: (h) 5 mA g^{-1} ; (k) 30 mA g^{-1} ; (l) 150 mA g^{-1} .

shows the ex situ attenuated total reflectance infrared (ATR-IR) spectra of the electrodes at the different charged and discharged states. The adsorption band around 900 cm^{-1} , which is associated with SiO_4^{4-} [14], is observable in all spectra from (a) to (g), confirming the existence of the orthosilicate group SiO_4^{4-} , which remained upon charging or discharging processes. However, Fig. 5B unambiguously shows that the width of the bands expanded in the spectra from (b) to (g) as compared to that of the uncharged one (a). It is well known that the adsorption bands in the IR spectra of an amorphous material were wider than those of the corresponding material in the crystal form [15]. Thus the results of the ex situ IR provided evidence for the changes of the materials from the crystalline state to an amorphous state, in line with the result of the ex situ XRD, which showed the disappear-

ance of the characteristic diffraction peaks associated with the crystalline $\text{Li}_2\text{MnSiO}_4$. Based on the ex situ experiments, we conclude that the crystalline $\text{Li}_2\text{MnSiO}_4$ changed to an amorphous state rather than decomposed into other compounds on the first charge and the followed electrochemical performance was that of the amorphous orthosilicates. This result is consistent with that of Dominko et al.'s [16]. On the first charging, Mn^{2+} changed to a mixture of Mn^{3+} and Mn^{4+} . The Jahn-Teller distortion associated with the Mn^{3+} should cause a big change in the lattice parameters and destroy the crystalline structure of the materials. This is quite different from the performances of $\text{Li}_2\text{FeSiO}_4$ [7], where the crystal structure did not collapse during the electrochemical process. Thus we infer that the poor cycling performance of the materials is associated with the Jahn-

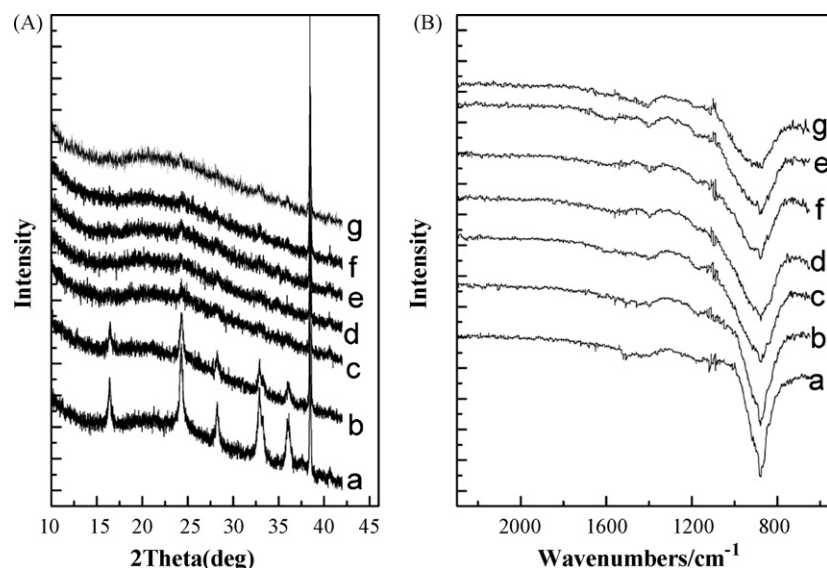


Fig. 5. XRD patterns (A) and ATR-IR spectra (B) of electrodes: (a) uncharged; (b) charged to 4.2 V; (c) charged to 4.5 V; (d) charged to 4.8 V; (e) discharged to 3.2 V; (f) discharged to 2.8 V; (g) discharged to 1.5 V.

Teller effect of Mn^{3+} , which caused the volumetric effect and destroyed the structure of the materials.

4. Summary

A high capacity Li_2MnSiO_4/C cathode material with good rate performance for lithium ion batteries has been successfully prepared and characterized with different techniques. We demonstrated, for the first time, that more than one electron exchange (about 1.25 electrons in the first charge/discharge cycle) can be reversible cycled in the orthosilicate system. The main reason for the good performance of the composite materials is due to the improvement of the electronic conductivity of the composite materials. Our results strongly suggest that silicates such as Li_2MnSiO_4 are promising cathode materials with good performance of high capacity, as well as safety.

Acknowledgments

This work was financially supported by the National Natural Science Foundation of China (nos. 29925310, 20473060, 20021002), and the Ministry of Science and Technology of China (2001CB610506).

References

- [1] J.M. Tarascon, M. Armand, *Nature* 414 (2001) 359.
- [2] Z.R. Zhang, Z.L. Gong, Y. Yang, *J. Phys. Chem. B* 108 (2004) 17546.
- [3] A.K. Padhi, K.S. Nanjundaswamy, J.B. Goodenough, *J. Electrochem. Soc.* 144 (1997) 1188.
- [4] A. Nyten, A. Abouimrane, M. Armand, T. Gustafsson, J.O. Thomas, *Electrochem. Commun.* 7 (2005) 156.
- [5] A.S. Prakash, P. Rozier, L. Dupont, H. Vezin, F. Sauvage, J.M. Tarascon, *Chem. Mater.* 18 (2006) 407.
- [6] R. Dominko, M. Bele, M. Gaberscek, A. Meden, M. Remskar, J. Jamnik, *Electrochem. Commun.* 8 (2006) 217.
- [7] A. Nyten, S. Kamali, L. Haggstrom, T. Gustafsson, J.O. Thomas, *J. Mater. Chem.* 16 (2006) 2266.
- [8] Y. Yang, Y.X. Li, Z.L. Gong, Abstract 210, in: IMLB2006, Biarritz, France, June 18–23, 2006.
- [9] Y. Yang, Y.X. Li, Z.L. Gong, Chinese Patent Application, 200610005329.2.
- [10] H.S. Liu, Z.R. Zhang, Z.L. Gong, Y. Yang, *Solid State Ionics* 166 (2004) 317.
- [11] M. Setoguchi, *Osaka Kogyo Gijustu Shikensho Hokoku* 374 (1988) 1.
- [12] J.C. Carver, G.K. Schweitzer, *J. Chem. Phys.* 57 (1972) 973.
- [13] L. Black, A. Stumm, K. Garbev, P. Stemmermann, K.R. Hallam, G.C. Allen, *Cem. Concrete Res.* 33 (2003) 1561.
- [14] A.M. Pires, M.R. Davolos, *Chem. Mater.* 13 (2001) 21.
- [15] J. Lin, D.U. Sanger, M. Mennig, K. Barner, *Thin Solid Films* 360 (2000) 39.
- [16] R. Dominko, M. Bele, A. Kokalj, M. Remskar, M. Gaberscek, J. Jamnik, Abstract 214, in: IMLB2006, Biarritz, France, June 18–23, 2006.